Journal of Biomaterials Science, Polymer Edition

ISSN: 0920-5063 (Print) 1568-5624 (Online) Journal homepage: https://www.tandfonline.com/loi/tbsp20

Nuclear targeting peptide-modified, DOX-loaded, PHBV nanoparticles enhance drug efficacy by targeting to Saos-2 cell nuclear membranes

Ayla Şahin, Gozde Eke, Arda Buyuksungur, Nesrin Hasirci & Vasif Hasirci

To cite this article: Ayla Şahin, Gozde Eke, Arda Buyuksungur, Nesrin Hasirci & Vasif Hasirci (2018) Nuclear targeting peptide-modified, DOX-loaded, PHBV nanoparticles enhance drug efficacy by targeting to Saos-2 cell nuclear membranes, Journal of Biomaterials Science, Polymer Edition, 29:5, 507-519, DOI: 10.1080/09205063.2018.1423812

To link to this article: https://doi.org/10.1080/09205063.2018.1423812

Published online: 12 Jan 2018.

JOURNAL OF BIOMATERIALS SCIENCE, POLYMER EDITION, 2018
VOL. 29, NO. 5, 507–519
https://doi.org/10.1080/09205063.2018.1423812

Taylor & Francis
Taylor & Francis Group

Nuclear targeting peptide-modified, DOX-loaded, PHBV nanoparticles enhance drug efficacy by targeting to Saos-2 cell nuclear membranes

Ayla Şahin[a,b], Gozde Eke[a,b,c], Arda Buyuksungur[b], Nesrin Hasirci[a,b,d] and Vasif Hasirci[a,b,e]

[a]Department of Biotechnology, Middle East Technical University (METU), Ankara, Turkey; [b]BIOMATEN, METU Center of Excellence in Biomaterials and Tissue Engineering, Ankara, Turkey; [c]Faculty of Arts and Sciences, Department of Chemistry, Ahi Evran University, Kirsehir, Turkey; [d]Department of Chemistry, Middle East Technical University (METU), Ankara, Turkey; [e]Department of Biological Sciences, Middle East Technical University (METU), Ankara, Turkey

ABSTRACT

The aim of this study was to target nano sized (266 ± 25 nm diameter) poly(3-hydroxybutyrate-co-3-hydroxyvalerate) (PHBV) particles carrying Doxorubicin (DOX), an anticancer agent, to human osteosarcoma cells (Saos-2). A nuclear targeting molecule (Nuclear Localization Signal, NLS), a 17 a.a. peptide, was attached onto the doxorubicin loaded nanoparticles. NLS conjugated nanoparticles surrounded the cell nuclei, but did not penetrate them. Free doxorubicin and doxorubicin loaded nanoparticles entered the cytoplasm and were evenly distributed within the cytoplasm. The localization of the NLS-targeted particles around the nuclear membrane caused a significantly higher decrease in the cancer cell numbers due to apoptosis or necrosis than the untargeted and free doxorubicin formulations showing the importance of targeting the nanoparticles to the nuclear membrane in the treatment of cancer.

ARTICLE HISTORY
Received 31 October 2017
Accepted 2 January 2018

KEYWORDS
PHBV; biodegradable nanoparticles; nuclear drug delivery; doxorubicin; nuclear localization signal

1. Introduction

Targeted drug delivery systems are important since they decrease the side effects by concentrating the drug at the desired site in the body [1,2]. The use of nanoparticles as drug carriers and as targeting agents has been increasing because of their ability to penetrate sites not accessible to larger particles and their large surface area-to-volume ratios that increases the drug release rates and lead to build up of drug concentration at the targeted tissue. The important component of a targeted delivery system is the 'targeting moiety' which helps to accumulate the drug at the appropriate site due to its specific interaction capability with certain groups or receptors at the target site [3–5]. Targeting could aim a tissue, an organ or an organelle. If the target is a nuclear component then, in order to increase the effectiveness, the targeting approach should entail attaching to or penetrating the nuclear membrane.

CONTACT Vasif Hasirci vhasirci@metu.edu.tr

Mammalian cells are highly compartmentalized and membrane bound structures. Thus, upon entry of the drug molecules into the cytosol, they are quickly distributed among the compartments according to the property of the drug and intracellular environment. Due to their small size, nanoparticles can cross the cell membrane and escape the endosomal/lysosomal pathway and enable the drug to be specifically carried to certain compartments [6,7]. According to He et al. (2016), the transfer of nanoparticles across cell membranes depends on the size, charge and shape [8]. Their results showed that carrier shapes with high aspect ratios have a higher chance of attaching to cell membranes and become internalized by the cancer cells. The surface charge of nanoparticles also affects the attachment to cell membrane through electrostatic interactions. The local interaction between the cell membrane and the part of the nanoparticle in contact with the cell membrane also plays a crucial role in endocytosis [8]. The positively charged nanoparticles interact with the negatively charged moieties on the cell membrane and this leads to bending of the membrane causing endocytosis and cellular uptake [9].

The nucleus is separated from the rest of cytoplasm by the double membrane structure of the nuclear envelope (NE) which constitutes a major barrier and the main rate limiting step in the transport of drugs into the nucleus [6,10]. The NE contains nuclear pore complexes (NPC) which are channels that allow the passive diffusion of small molecules (ca. 9 nm in diameter) or transport of larger molecules (ca. 39 nm in diameter) in an energy dependent manner [4]. The transfer of drugs through the energy dependent pathway into the nucleus is mediated by homologous proteins called importins. This transfer mechanism is divided into two steps. In the first step, importin α binds to Nuclear Localization Signal (NLS), which is a special oligopeptide, and importin β binds to the cytoplasmic filaments that bring the target molecule to the nuclear pore. In the second step, importin α is transported through the nuclear pore into the nucleus together with its cargo [11].

Chemotherapy has been a major therapeutic approach for the treatment of cancer. Doxorubicin (DOX) is a widely used anticancer agent for bone cancer treatment and has also shown activity against the solid tumors with its action inside the nucleus. It has an anthracycline structure and is isolated from a soil bacterium, *Streptomyces peucetius*. In general, anthracycline drugs prefer to intercalate the DNA base pairs that are connected to sugar moieties in the DNA minor groove and prevent resealing of DNA during the replication and transcription, and interrupt cell division. DOX interacts with both healthy and cancerous cells causing undesirable side effects. Nanotechnology is an approach that could increase the activity of DOX by maximizing its effect by concentrating it at the cancerous tissue and minimizing its damage to healthy sites [11,12].

In this study, DOX loaded poly(3-hydroxybutyric acid-co-3-hydroxyvaleric acid) (PHBV) nanoparticles were designed to serve as an anticancer drug delivery system. NLS was conjugated on the nanoparticles to target them to the nucleus with the purpose of increasing the cytotoxic effect of the drug *in vitro*. Even though the transfer of the nanoparticles with sizes higher than 50 nm into the nucleus is not expected, their attachment to the nuclear membrane would concentrate the anticancer agent around the nucleus and increase its effect. Nile Red was used as a fluorescent dye in order to observe *in vitro* cell penetration of nanoparticles in the absence of DOX. Human osteosarcoma cells (Saos-2) were used to study the cytotoxic effect of DOX delivered with the nanoparticles. The encapsulation efficiency (EE), *in situ* drug release kinetics, cytotoxicity and cell penetration of the nanoparticles

were determined under *in vitro* conditions. Apoptotic trends due to DOX were studied by measuring the activity of FITC-Annexin V and Propidium Iodide with flow cytometry.

2. Materials and methods

2.1. Preparation of nanoparticles

In this study, we prepared two different types of nanoparticles; nanocapsules and nanospheres. We used the nanocapsules to deliver DOX, a water-soluble drug, and the nanospheres which were stained with Nile Red (a hydrophobic stain) to be used in cell permeation studies as fluorescent particles.

2.1.1. Preparation of DOX loaded PHBV nanocapsules

Water-in-oil-in-water ($w_1/o/w_2$) emulsion technique was used for the production of DOX loaded nanocapsules (NP-DOX) [13]. Briefly, DOX solution (Sigma, USA) in water (200 µL, 1 mg/mL) was added into a solution of PHBV (HV content 11% M) (Sigma, USA) in chloroform (0.6 mL, 10% *w*/*v*). This mixture was added into an aqueous solution of polyvinyl alcohol (PVA, MW 1.5×10^4, 2 mL, 4% *w*/*v*) (Fluka, USA) and sonicated for 30 s in an ice bath. This emulsion was added into another PVA solution (50 mL, 0.3% *w*/*v*). Chloroform was then evaporated by stirring, and nanoparticles were collected by centrifugation (23,000 g, 20 min), washed with distilled water (dH_2O), frozen at −20 °C and lyophilized.

2.1.2. Preparation of Nile Red stained PHBV nanospheres

Oil-in-water (*o*/*w*) technique was used for the production of Nile Red loaded PHBV nanospheres (NP-NLR). For this purpose, a hydrophobic dye, Nile Red (0.1 mL, 0.01% in acetone) (Sigma, USA) was added into the solution of PHBV in chloroform and the procedure was then completed as mentioned above. In order for consistency the word 'nanoparticles' was used to represent both the nanocapsules and nanospheres throughout the text.

2.3. NLS conjugation on PHBV nanoparticles

PHBV nanoparticles (10 mg) were suspended in ultrapure water (6 mL). In order to activate the nanoparticle surface, aqueous EDC (300 µL, 1 mg/mL) and NHS (300 µL, 1 mg/mL) solutions were added to the PHBV nanoparticle suspension and stirred for 1 h at 37 °C. Then, this suspension was centrifuged (23,000 g, 20 min). The precipitate containing surface activated PHBV nanoparticles was suspended in a solution of 17 amino acid oligopeptide NLS (DRQIKIWFQNRRMKWKK, Thermo Scientific USA), incubated for 1 h at room temperature, frozen at −20 °C and lyophilized.

2.4. Particle size of PHBV nanoparticles

Size of the PHBV nanoparticles was studied with scanning electron microscopy (QUANTA 400F Field Emission SEM, Netherlands). The mean diameter was measured from the SEM micrographs using the Image J program (NIH, USA).

Size distribution curves of PHBV nanoparticles were obtained with a Malvern Zetasizer (Nano ZS90, UK).

2.5. Loading and encapsulation efficiency (EE) of DOX

DOX loaded PHBV nanocapsules (20 mg) were dissolved in chloroform and the drug was extracted with distilled water. The total amount of DOX in the aqueous layer was measured with a spectrofluorimeter (Molecular Devices, SpectraMax M2, USA). The fluorescence intensity values (λ_{ex}: 480 nm, and λ_{em}: 590 nm) were converted into percentage values using a calibration curve.

The values for loading and EE were calculated by using the following equations [13];

$$\text{Loading } (\%) = \left[\text{Amount of encapsulated DOX } (\text{mg}) / \text{Total amount of NP } (\text{mg})\right] \times 100 \quad \text{(I)}$$

$$\text{EE}\,(\%) = \left[\text{Amount of encapsulated DOX } (\text{mg}) / \text{Input amount of DOX} (\text{mg})\right] \times 100 \quad \text{(II)}$$

2.6. In situ DOX release from nanoparticles

Nanoparticles were suspended in ultrapure water (3 mL, 20 mg/mL) and placed in a dialysis tubing (Snake skin, cut off MW 10,000, Thermo Scientific, USA). The tubings were placed in ultrapure water 10 mL and stirred on a magnetic stirrer at 37 °C for 35 days. At various time points, fluorescence of the released DOX was measured by using a spectrofluorometer. For this purpose, 200 µL of solution was removed from the dialysis medium (from outside the dialysis bag), added into 96 well plates and spectrofluorometric reading was made at λ_{ex}: 480 nm, and λ_{em}: 590 nm. The solutions were returned to the dialysis medium. The data was plotted as 'released DOX amount (%) vs. time' (M_t vs. t) and also according to Higuchi Equation (M_t/M_∞ vs. $t^{1/2}$), where Mt is the amount of DOX released at a given time and M_∞ is the total released amount.

2.7. X-ray photoelectron spectroscopy (XPS) analysis

The presence of NLS on PHBV nanoparticles was represented by the existance of nitrogen in the samples since PHBV does not contain any nitrogen. X-ray Photoelectron Spectroscopy measurements were performed using XPS-PHI (PHI 5000 VersaProbe, USA) that uses a monochromatic Al X-ray source. For each sample, a survey scan was obtained and especially the regions for nitrogen (390–410 eV) and carbon (280–305 eV) were examined.

2.8. In vitro studies

2.8.1. Effect of free DOX and DOX loaded nanoparticles on cell proliferation

The toxic effect of different concentrations of free DOX on proliferation of Saos-2 cells was studied using an Alamar Blue assay. Cells (2×10^4/well) (passages 10 to 15) were seeded in 24-well plates. After cell attachment, RPMI medium (Lonza, Switzerland) was replaced with free DOX dissolved in culture medium with final concentrations in the range of 0.01–100.00 µg/mL. On Day 4, the cells were washed twice with PBS (10 mM, pH 7.4) and incubated in 10% Alamar Blue solution in DMEM colorless growth medium for 1 h at 37 °C in a 5% CO_2 incubator. The absorbances of this solution (200 µL) were determined at 570 and 595 nm by using Elisa Plate Reader (Molecular Devices, USA) and converted into cell numbers using a calibration curve.

Similar procedure was applied using nanoparticles incubated with Saos-2 cells. Cells (2.5×10^4 /well) were incubated with nanoparticles (4 mg/mL) in 10% Alamar Blue solution in DMEM colorless medium for 24 h at 37 °C under a 5% CO_2 atmosphere. The control group had only Saos-2 cells, and did not contain any nanoparticles. On Day 4, similar procedure was followed to measure the number of cells.

2.8.2. Determination of apoptotic cells by flow cytometry

Apoptosis of Saos-2 cells was studied by flow cytometry. Cells were seeded in 6 well plates and incubated for 2 h at 37 °C and exposed to DOX drug, DOX loaded and unloaded nanoparticles in the RPMI medium and incubated for 24 h at 37 °C. The cells were then centrifuged (5000 g for 5 min) and suspended in fluorescence-activated cell sorting (FACS) buffer followed by centrifugation and resuspension with Annexin V Binding Buffer. FITC-Annexin and propidium iodide solutions were added and incubated at room temperature for 15 min. The remaining suspension was analyzed by FACScan flow cytometer (BD Accuri C6 Plus, USA). The percentage of apoptotic cells was determined for each sample.

2.8.3. Intracellular localization of PHBV nanoparticles in Saos-2 cells

Interactions of nanoparticles with Saos-2 cells were studied using confocal laser scanning microscopy (CLSM). Cells were seeded into 6 well plates containing nanoparticles (4 mg/mL) and were incubated in RPMI medium (24 h, 37 °C). Cells were then washed with PBS, fixed with paraformaldehyde (4%, 1 mL), and stained with Draq5 and Alexa Fluor 488-Phalloidin for nucleus and cytoskeleton, respectively. They were then examined with CLSM (Leica DM2500, Germany).

2.9. Statistical analysis

All experiments were carried out in triplicates. Significant differences between mean values in control and test groups were determined using one way ANOVA with Tukey's post hoc test. Means were considered to be significantly different for $p \leq 0.05$ values.

3. Results and discussion

3.1. Nanoparticle characterization: dimension, encapsulation efficiency and loading

PHBV nanoparticles were produced by dissolving 10% (*w*/*v*) polymer solution in chloroform. The concentration was selected based on our earlier studies conducted with the same polymer [13,14]. Nano sized particles with smooth surfaces were obtained.

Using SEM micrographs and NIH ImageJ program, the average diameters of unloaded (Figure 1(A)), Nile Red loaded (Figure 1(B)), DOX loaded (Figure 1(C)) and NLS conjugated DOX loaded PHBV nanoparticles were determined as 206 ± 14, 266 ± 5, 219 ± 17 and 266 ± 12 nm, respectively. Size distribution of these nanoparticles is also presented in Figure 1(D). These show that the nanoparticle size did not change considerably due to the conjugation of NLS onto the surface. Misra et al. (2010) previously showed that PLGA nanoparticles did not significantly increase in size after the conjugation of NLS onto their nanoparticles supporting our result (226 vs. 234 nm) [7]. The size of DOX loaded PHBV

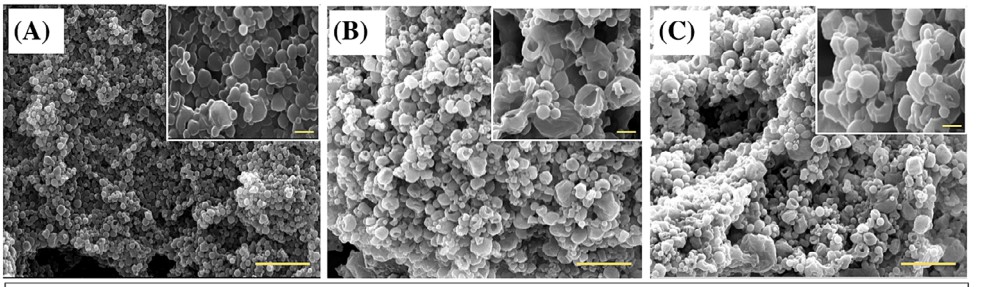

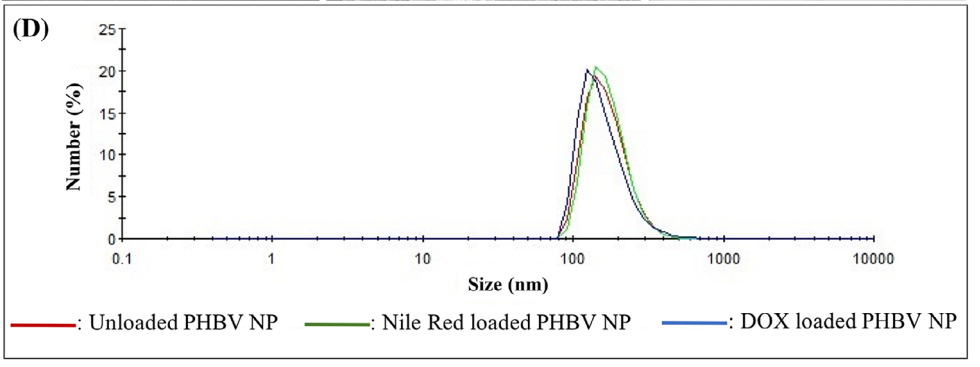

(E)	Unloaded NP	Nile Red Loaded NP	DOX Loaded NP	DOX Loaded NLS Conjugated NP
Av. Size (nm)	206± 14	266± 5	219± 17	266± 12
PDI	0.1	0.3	0.4	0.3
Loading (%)	-	-	13.5± 0.5	-
EE (%)	-	-	22.9± 1.7	-

Figure 1. Characterization of PHBV Nanoparticles. SEM images of (A) unloaded, (B) Nile Red loaded, (C) DOX loaded Nanoparticles. Unloaded PHBV nanoparticles showed round and smooth surfaces (Magnification: 10,000x, Scale bar: 5 μm). Nile Red and DOX loaded PHBV nanoparticles were spherical in shape. Insets show close ups of the nanoparticles (Magnification: 40,000x. Scale bar: 1 μm). (D) Size distribution of unloaded, Nile Red and DOX loaded Nanoparticles. (E) Average sizes, loading and encapsulation efficiency of Nile Red, DOX and NLS-DOX Loaded Nanoparticles (Please see the online article for the colour version of this figure: https://doi.org/10.1080/09205063.2018.1423812).

nanoparticles were not monodisperse, so there were particles smaller than 100 nm which had the potential to cross into the nucleus through the nuclear pores.

The loading of the drug, DOX, into the particles was achieved by water-in-oil-in-water ($w_1/o/w_2$) emulsion technique where the drug is encapsulated into the core of PHBV nanocapsules. The encapsulation efficiencies and the loading values of the particles for DOX were 22.9 ± 1.7 and 13.5 ± 0.5%, respectively (Figure 1(E)). In a previous study [15], PLGA nanoparticles prepared by solvent evaporation and loaded with DOX had a similar value for encapsulation efficiency (22.0 ± 0.8%). In solvent evaporation method, the solvent that was used to dissolve PLGA polymer was evaporated overnight, which was similar to the method in this study. In another study [16], DOX loaded PHBV nanoparticles were prepared

by solvent displacement method and had an encapsulation efficiency of 74.0 ± 5.4% and a loading of 7.9 ± 0.2%. The mean diameter of the nanoparticles was 396 ± 7 nm. In that study, the encapsulation efficiency is higher but the loading is lower than the present study. This indicates that they would need to use a higher amount of nanoparticles to achieve the same dose with our nanoparticles which is shown to be detrimental on cell survival [14].

3.2. X-ray photoelectron spectroscopy (XPS) analysis

The chemistry of empty PHBV nanoparticles with and without NLS conjugation were studied with X-ray photoelectron spectroscopy (XPS) in order to show the presence of NLS on the nanoparticles. NLS is a small oligopeptide composed of 17 amino acids and carries nitrogen due to the peptide bonds whereas PHBV consists of only C, H and O. Thus, detection of nitrogen proves the presence of peptides. NLS loaded nanoparticles showed the presence of nitrogen. Uncoated PHBV nanoparticles had 67.4% C and 32.6% O whereas PHBV nanoparticles conjugated with NLS had 67.4% C, 30.9% O and 1.8% N in their structures proving the presence of the peptide coat (Figure 2(A)).

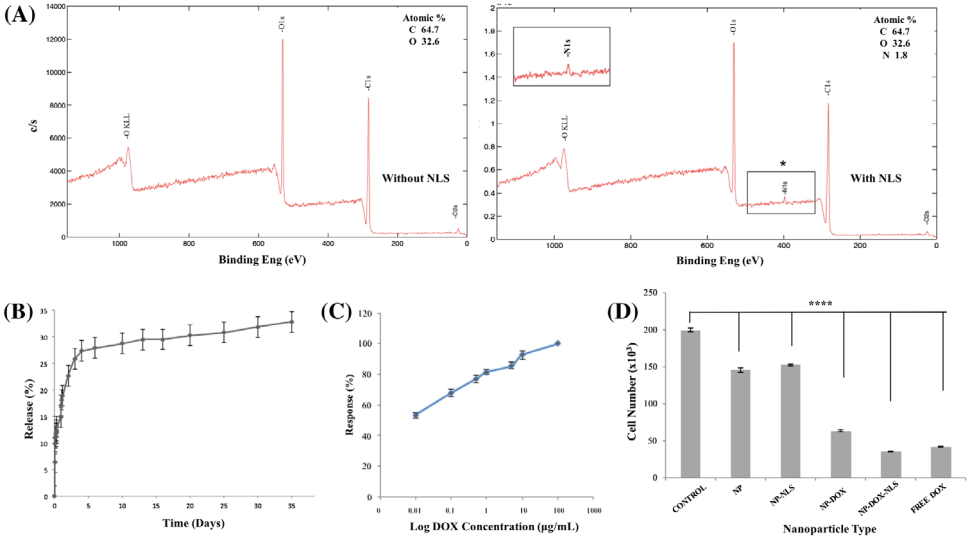

Figure 2. (A) The XPS data of empty PHBV nanoparticles with and without NLS conjugation. (B) *In situ* release of DOX from PHBV nanocapsules. Quantification was made by measuring the DOX concentration in ultrapure water at 37 °C ($n = 3$). (C) Antiproliferative effect of free DOX on Saos-2 cell viability measured by Alamar Blue assay on day 4 after exposure to the drug at 37 °C. Initial seeding density: 2×10^4 cells/sample. (D) Effect of PHBV nanoparticles on Saos-2 cell proliferation was determined by Alamar Blue assay ($n = 3$). Untreated cells were used as the control group. Cells treated with empty nanoparticles (NP), NLS conjugated nanoparticles (NP-NLS), DOX loaded nanoparticles (NP-DOX), NLS conjugated and DOX loaded nanoparticles (NP-DOX-NLS) and free DOX were incubated at 37 °C for 4 days. Initial seeding density: 2.5×10^4 cells/sample (ANOVA One-Way Tukey test, ****$p < 0.001$) (Please see the online article for the colour version of this figure: https://doi.org/10.1080/09205063.2018.1423812).

3.3. In situ release of DOX

The *in situ* release behavior of DOX loaded PHBV nanoparticles presents a Zero Order Kinetics (cumulative release (%) vs. time plot) (Figure 2(B)) It is observed that the nanoparticles show a rapid release of 27% in 5 days. This release could be due to the drug that is adsorbed or attached ionically on the surface of nanoparticles. During the second phase, the release was slower and followed zeroth order kinetics (ca. 1 μg/day) leading to a total of 35% release in 35 days. In a similar study [17], it was reported that DOX loaded PLGA nanoparticles released 63% of DOX in 60 days in a sustained release manner similar to the present study. In another study [18] magnetic silica nanoparticles carrying DOX and coated with PLGA released 60% in 5 days, a very rapid release unsuitable for controlled delivery. Thus, the controlled release rate of DOX in this study is comparable to those presented in the literature and very suitable for delivering DOX to cancer cells in a controlled fashion.

3.4. In vitro tests

3.4.1. Effect of DOX on cell proliferation

The effect of free DOX on proliferation of Saos-2 cells was studied by measuring the viability of the cells when exposed to the drug solution with concentrations in the range 0.01–100.0 μg/mL (Figure 2(C)). The results show that DOX has a significant antiproliferative effect on Saos-2 cells in a concentration dependent manner where the 'Response (percent of dead cells) vs. log DOX' was linear. According to the literature [11,18] a dose of 100 μg/mL (3.5 g/m^2), is extremely effective clinically on cancer cells.

3.4.2. Effect of DOX released from nanoparticles on Saos-2 cell viability

In the literature, it is reported that IC50 for DOX on Saos-2 cell line is 37 ± 16 nM, and this corresponds to 0.58 μg DOX [19]. DOX effectiveness tests were carried out where samples carrying 0.58 μg DOX were added to the culture plates for 25,000 cells. The effect of nanoparticles on Saos-2 proliferation was studied using 4 groups of nanoparticles: Unloaded PHBV nanoparticles (NP); Unloaded PHBV nanoparticles conjugated with NLS (NP-NLS); PHBV nanoparticles loaded with Doxorubicin (NP-DOX) and PHBV nanoparticles loaded with DOX and conjugated with NLS (NP-DOX-NLS). Free DOX was used as the control. After 4 days of exposure, the cell number was determined with Alamar Blue assay. Figure 2(D) shows the effect of DOX released from each sample on cell proliferation. Nuclear membrane targeted NP-DOX-NLS and free DOX caused the highest reduction in cell numbers while untargeted nanoparticles carrying DOX (NP-DOX) showed the lowest decrease (35,000 and 41,000 vs. 63,000) in cell number. The difference in cell number for all samples and the control were statistically significant (****$p < 0.001$). This shows that conjugation of the nanoparticles with NLS had a significant impact on the delivery of DOX towards the nucleus. The data also shows that NLS conjugated nanoparticles were more effective in delivering the DOX than the free drug indicating the importance of the targeting step. Drug free NP and NP-NLS treated samples showed similar cell numbers, around 25% lower than the untreated control cells, indicating that the nanoparticles might have led to some decrease in the cell numbers.

3.4.3. Determination of apoptotic cells by flow cytometry

Cytotoxicity caused by DOX is classified as apoptosis and as necrosis since it is known that DOX can cause cell death by both these mechanisms [20–22]. Apoptosis (programmed cell death) is an active process that involves condensation of chromatin, shrinkage of cell, fragmentation of nucleus and results in cell death whereas necrosis (unexpected or accidental cell death) involves cell and mitochondria swelling, cause disruption of cell membrane and result in a late apoptosis stage [23,24]. These two modes of cell death were measured using FITC-Annexin-V and Propidium Iodide. Cells that were not stained with either FITC-Annexin-V or Propidium Iodide were non-apoptotic, non-necrotic, or in other words live, healthy cells. On the other hand, cells that were stained with Propidium Iodide but not with FITC-Annexin-V were necrotic cells; cells that were stained with only FITC-Annexin-V were early apoptotic, and finally cells that were stained positive for both were late apoptotic cells. Gating was performed according to forward and side scatter plot (Figure 3(A)). Untreated cells (Figure 3(B)) and cells treated with empty (DOX-free) PHBV nanoparticles showed similar flow cytometry scattering patterns (around 3% necrotic, 4% early apoptotic and 1% late apoptotic). This indicates that the presence of nanoparticles does not have a significant effect on cell proliferation (Figure 3(B) and (C)). On the other hand, 98.7% of the cells treated with free DOX, were in late apoptotic phase and 0.25% were necrotic (Figure 3(D)). Cells treated with untargeted NP-DOX were significantly less affected than cells treated with targeted NP-DOX-NLS. The values are 22% late apoptotic and 77% necrotic (Figure 3(E)) compared to 72% late apoptosis, and 28% necrosis (Figure 3(F)), respectively.

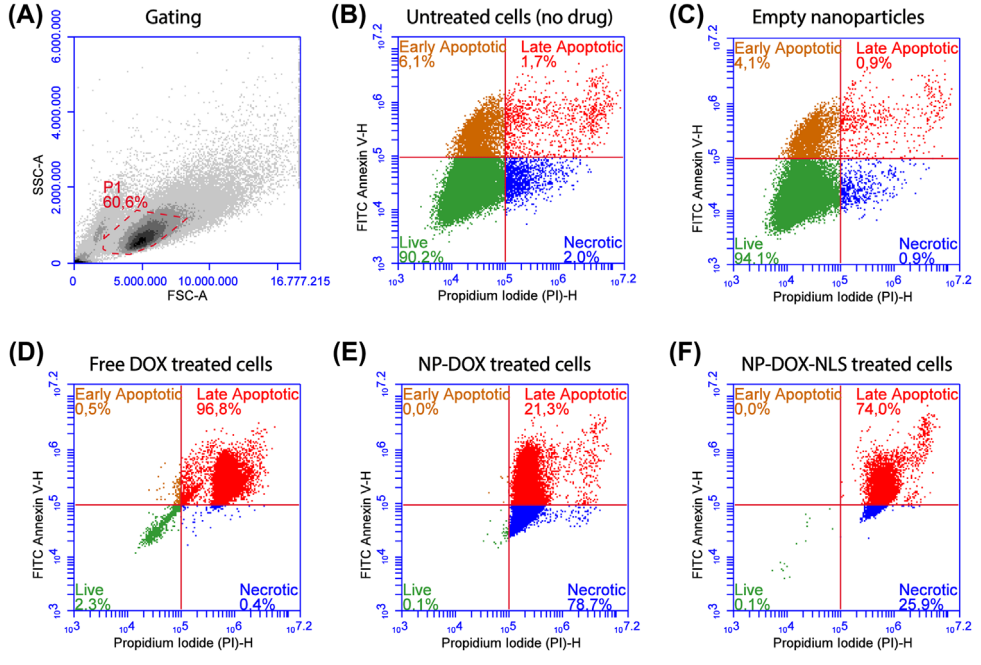

Figure 3. Study of apoptosis and necrosis of Saos-2 cells after treatment with DOX as measured with flow cytometry. (A) Gating of the cell population (B) Untreated cells. Cells treated with (C) empty PHBV nanoparticles, (D) Free DOX, and (E) DOX loaded nanoparticles, (F) NLS conjugated and DOX loaded nanoparticles. Cells were incubated for 24 h at 37 °C. Initial seeding density: 5×10^5 cells /sample.

This shows that the conjugation of NLS onto the PHBV nanoparticles increased the proportion of apoptotic cells indicating the effectiveness of targeting by NLS. Thus, the flow cytometric studies distinctly show that DOX causes apoptosis in Saos-2 cells and targeting with NLS result in significantly more cells to go into late apoptosis.

3.4.4. Intracellular localization of PHBV nanoparticles in Saos-2 cells

The actin filaments of the cytoskeleton of Saos-2 was stained with FITC-Phalloidin and the cell nuclei with Draq5. Nile Red (NLR) is a hydrophobic, fluorescent dye and was used to stain the PHBV nanoparticles. CLSM showed that the control (untreated) cells showed no signs of particles (Figure 4(A)). Cells treated with PHBV nanoparticles were also examined

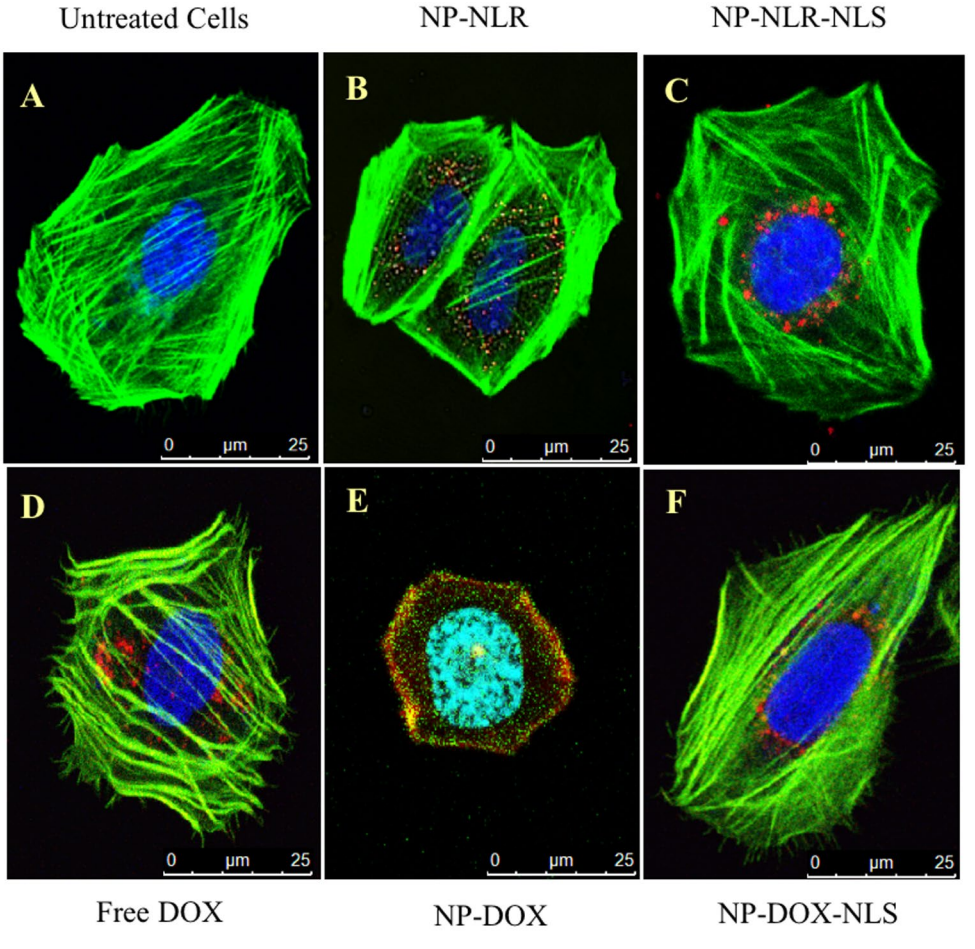

Figure 4. Confocal microscopy of the interaction of nanoparticles with Saos-2 cells. (A) Control group; untreated cells. Cells were treated with (B) Nile Red loaded nanoparticles (NP-NLR), and (C) NLS conjugated and Nile Red loaded nanoparticles (NP-NLR-NLS). The cells were stained with FITC-Phalloidin for the cytoskeleton. Cells were treated with: (D) Free DOX, (E) DOX loaded nanoparticles (NP-DOX), and (F) NLS conjugated and DOX loaded nanoparticles (NP-DOX-NLS). The cell cytoskeleton was stained with Alexa Fluor 488-Phalloidin. Nanoparticles were visible as red specks due to the Nile Red dye or DOX. All the cells were stained with Draq5 for the nucleus and they were incubated for 24 h at 37 °C (Please see the online article for the colour version of this figure: https://doi.org/10.1080/09205063.2018.1423812).

with CLSM. Figures 4 (D), (E) and (F) show significant amounts of DOX taken up by Saos-2 cells during 24 h incubation. Targeted nanoparticles (NP-NLR-NLS) (C) and NP-DOX-NLS (F) were localized around the cell nucleus probably guided by the NLS while the untargeted nanoparticles were randomly dispersed in the cytoplasm (Figures 4 (B) and (E)).

The volume of the cytoplasm of free DOX treated cells were decreased (Figure 4(E)). Saos-2 cells treated with NP-DOX-NLS showed that the nanoparticles successfully crossed the plasma membrane and accumulated around the nucleus (Figure 4(F)). Eke et al. (2015) showed that the fibroblastic cells take up low (200 nm) and mid-nano (420 nm) sized PHBV particles in the cytoplasm, however, the low-micro sized (2 μm) particles were unable to penetrate into the cytoplasm [14]. Tkachenko et al. (2004) reported NLS conjugated gold nanoparticles with a diameter of 20 nm were able to cross the nuclear membrane of HeLa cells due to their small size [25]. In another study by Cheng et al. (2008), quantum dot carrying PLGA nanoparticles conjugated with NLS and had a diameter of 72 nm were taken up by HeLa cells and delivered into the nucleus [26]. Park et al. (2016) demonstrated that Apelin-17 peptide conjugated PLGA nanoparticles with a diameter of 120 nm were able to pass through the human mesenchymal stem cell (hMSC) membrane and deliver their content into the nucleus [27]. However, in our study, even though the targeted nanoparticles surrounded and interacted with the nuclear membrane they were not small enough to cross into the nucleus.

Another observation with CLSM is the cell membrane of the cytoplasm of Saos-2 cells (Figure 4(E) and (F)) indicating that DOX molecules were effectively delivered into the nucleus. The main action of DOX on cancer cells is based on inhibition of Topoisomerase II which causes the generation of free radicals. These free radicals damage proteins, DNA and the membranes inducing apoptosis through cleavage of DNA and formation of hydrogen peroxide [21,28]. According to the literature, since the cells cannot go through replication due to the intercalation of DNA by DOX, they may go through apoptosis or necrosis since the cell membrane is disrupted. Thus, the targeted nanoparticles carried their DOX cargo to the nuclear membrane, the DOX was released there and penetrated the nucleus and showed its apoptotic effect.

4. Conclusions

In this study, anticancer agent doxorubicin loaded PHBV nanoparticles were targeted to the nucleus of Saos-2 human osteosarcoma cells to increase the anticancer effect of the drug carried in biodegradable nanoparticles. Alamar Blue assay showed that the doxorubicin carried by the targeted nanoparticles decreased cell proliferation more than untargeted nanoparticles. Also, the targeted nanoparticles were more effective in causing apoptosis or necrosis than the untargeted. Even though the nanoparticles were not small enough to penetrate the nuclear membrane the targeting moiety led the nanoparticles to surround the nucleus indicating that targeting process was effective. The significant difference between the effect of the targeted and untargeted nanoparticles is probably caused by the NLS-targeted nanoparticles attaching to the nuclear membrane and released their DOX content near the nucleus where the target, the DNA, is located. In this context, it can be stated that the NP-DOX-NLS formulation developed in this study has a significant potential to be used as a targeted drug delivery system for the treatment of osteosarcoma especially if the particle sizes are smaller.

Disclosure statement

No potential conflict of interest was reported by the authors.

Funding

This work was financially supported by Middle East Technical University Center of Excellence in Biomaterials and Tissue Engineering (BIOMATEN).

References

[1] Crommelin DJ, Florence AT. Towards more effective advanced drug delivery systems. Int J Pharm.. 2013;454(1):496–511. doi:10.1016/j.ijpharm.2013.02.020.
[2] Lee JH, Yeo Y. Controlled drug release from pharmaceutical nanocarriers. Chem Eng Sci. 2015;125:75–84. doi:10.1016/j.ces.2014.08.046.
[3] Parhi P, Mohanty C, Sahoo SK. Nanotechnology-based combinational drug delivery: an emerging approach for cancer therapy. Drug Discovery Today. 2012;17:1044–1052. doi:10.1016/j.drudis.2012.05.010.
[4] Biswas S, Torchilin VP. Nanopreparations for organelle-specific delivery in cancer. Adv Drug Deli Rev. 2014;66:26–41. doi:10.1016/j.addr.2013.11.004.
[5] Bertrand N, Wu J, Xu X, et al. Cancer nanotechnology: the impact of passive and active targeting in the era of modern cancer biology. Adv Drug Deliv Rev. 2014;66:2–25. doi:10.1016/j.addr.2013.11.009.
[6] Pouton CW, Wagstaff KM, Roth DM, et al. Targeted delivery to the nucleus. Adv Drug Deliv Rev. 2007;59(8):698–717. doi:10.1016/j.addr.2007.06.010.
[7] Misra R, Sahoo SK. Intracellular trafficking of nuclear localization signal conjugated nanoparticles for cancer therapy. Eur J Pharm Sci. 2010;39(1–3):152–163. doi:10.1016/j.ejps.2009.11.010.
[8] He Y, Park K. Effects of the microparticle shape on cellular uptake. Mol Pharm. 2016;13(7):2164–2171. doi:10.1021/acs.molpharmaceut.5b00992.
[9] Uchechi O, Ogbonna JDN, Attama AA. Nanoparticles for dermal and transdermal drug delivery, application of nanotechnology in Drug Delivery. InTech. 2014. doi:10.5772/58672.
[10] Bagherifam S, Skjeldal FM, Griffiths G, et al. pH-responsive nano carriers for doxorubicin delivery. Pharm Res. 2015;32(4):1249–1263. doi:10.1007/s11095-014-1530-0.
[11] Hinde E, Thammasiraphop K, Duong HT, et al. Pair correlation microscopy reveals the role of nanoparticle shape in intracellular transport and site of drug release. Nature Nanotechnology. 2016;12:81–89. doi:10.1038/nnano.2016.160.
[12] Sarkar S, Osama K, Mohammad Sajid Jamal Q, et al. Advances and implications in nanotechnology for lung cancer management. Curr Drug Metab. 2017;18(1):30–38. doi:10.2174/1389200218666161114142646.
[13] Eke G, Goñi-de-Cerio F, Suarez-Merino B, et al. Biocompatibility of dead sea water and retinyl palmitate carrying poly (3-hydroxybutyrate-co-3-hydroxyvalerate) micro/nanoparticles designed for transdermal skin therapy. J Bioact Compat Polym. 2015;30(5):455–471. doi:10.1177/0883911515585183.
[14] Eke G, Kuzmina AM, Goreva AV, et al. In vitro and transdermal penetration of PHBV micro/nanoparticles. J Mater Sci: Mater Med. 2014;25:1471–1481. doi:10.1007/s10856-014-5169-5.
[15] Cui Y, Xu Q, Chow PKH, et al. Transferrin-conjugated magnetic silica PLGA nanoparticles loaded with doxorubicin and paclitaxel for brain glioma treatment. Biomaterials. 2013;34(33):8511–8520. doi:10.1016/j.biomaterials.2013.07.075.
[16] Chittasupho C, Lirdprapamongkol K, Kewsuwan P, et al. Targeted delivery of doxorubicin to A549 lung cancer cells by CXCR4 antagonist conjugated PLGA nanoparticles. Eur J Pharm Biopharm. 2014;88(2):529–538. doi:10.1016/j.ejpb.2014.06.020.

[17] Tewes F, Munnier E, Antoon B, et al. Comparative study of doxorubicin-loaded poly (lactide-co-glycolide) nanoparticles prepared by single and double emulsion methods. Eur J Pharm Biopharm. 2007;66(3):488–492. doi:10.1016/j.ejpb.2007.02.016.
[18] Mita MM, Natale RB, Wolin EM, et al. Pharmacokinetic study of aldoxorubicin in patients with solid tumors. Invest New Drugs. 2015;33(2):341–348. doi:10.1007/s10637-014-0183-5.
[19] Graat HC, Witlox M, Schagen FHE, et al. Different susceptibility of osteosarcoma cell lines and primary cells to treatment with oncolytic adenovirus and doxorubicin or cisplatin. Br J Cancer. 2006;94:1837–1844. doi:10.1038/sj.bjc.6603189.
[20] Wang S, Konorev E, Kotamraju S, et al. Doxorubicin induces apoptosis in normal and tumor cells via distinctly different mechanisms intermediacy of H2O2-and p53-dependent pathways. J Biol Chem. 2004;279(24):25535–25543. doi:10.1074/jbc.M400944200.
[21] Khazaei S, Ramachandran V, Abdul hamid Roslida N, et al. Flower extract of Allium atroviolaceum triggered apoptosis, activated caspase-3 and down-regulated antiapoptotic Bcl-2 gene in HeLa cancer cell line. Biomed Pharmacother. 2017;89:1216–1226. doi:10.1016/j.biopha.2017.02.082.
[22] Eom YW, Kim MA, Park SS, et al. Two distinct modes of cell death induced by doxorubicin: apoptosis and cell death through mitotic catastrophe accompanied by senescence-like phenotype. Oncogene. 2005;24(30):4765–4777. doi:10.1038/sj.onc.1208627.
[23] Wlodkowic D, Skommer J, Darzynkiewicz Z. Flow cytometry-based apoptosis detection. Methods Mol Biol. 2009;559:19–32. doi:10.1007/978-1-60327-017-5_2.
[24] Searle J, Kerr JF, Bishop CJ. Necrosis and apoptosis: distinct modes of cell death with fundamentally different significance. Pathol Annu. 1982;17:229–259.
[25] Tkachenko AG, Xie H, Liu Y, et al. Cellular trajectories of peptide-modified gold particle complexes: comparison of nuclear localization signals and peptide transduction domains. Bioconjug Chem. 2004;15(3):482–490. doi:10.1021/bc034189q.
[26] Cheng FY, Wang SPH, Su CH, et al. Stabilizer-free poly (lactide-co-glycolide) nanoparticles for multimodal biomedical probes. Biomaterials. 2008;29(13):2104–2112. doi:10.1016/j.biomaterials.2008.01.010.
[27] Park JS, Yang HN, Yi SW, Kim JH, Park KH. Neoangiogenesis of human mesenchymal stem cells transfected with peptide-loaded and gene-coated PLGA nanoparticles. Biomaterials. 2016;76:226–237. doi:10.1016/j.biomaterials.2015.10.062.
[28] Chettab K, Mestas JL, Lafond M, et al. Doxorubicin delivery into tumor cells by stable cavitation without contrast agents. Mol Pharm. 2017;14(2):441–447. doi:10.1021/acs.molpharmaceut.6b00880.